Accepted Manuscript

A novel biosorbent prepared by immobilized *Bacillus licheniformis* for lead removal from wastewater

Xiaofeng Wen, Chunyan Du, Guangming Zeng, Danlian Huang, Jinfan Zhang, Lingshi Yin, Shiyang Tan, Lu Huang, Hong Chen, Guanlong Yu, Xuyue Hu, Cui Lai, Piao Xu, Jia Wan

PII: S0045-6535(18)30280-7

DOI: 10.1016/j.chemosphere.2018.02.078

Reference: CHEM 20836

To appear in: *ECSN*

Received Date: 6 August 2017

Revised Date: 8 January 2018

Accepted Date: 12 February 2018

Please cite this article as: Wen, X., Du, C., Zeng, G., Huang, D., Zhang, J., Yin, L., Tan, S., Huang, L., Chen, H., Yu, G., Hu, X., Lai, C., Xu, P., Wan, J., A novel biosorbent prepared by immobilized *Bacillus licheniformis* for lead removal from wastewater, *Chemosphere* (2018), doi: 10.1016/j.chemosphere.2018.02.078.

A novel biosorbent prepared by immobilized *Bacillus licheniformis* for lead removal from wastewater

Xiaofeng Wen [a,b,c,d], Chunyan Du [a,b*], Guangming Zeng [c,d*], Danlian Huang [c,d], Jinfan Zhang [a,b], Lingshi Yin [a,b], Shiyang Tan [a,b], Lu Huang [c,d], Hong Chen [a,b], Guanlong Yu [a,b], Xuyue Hu [a,b], Cui Lai [c,d], Piao Xu [c,d], Jia Wan [c,d]

[a] School of Hydraulic Engineering, Changsha University of Science &Technology, Changsha 410114, P.R.China;

[b] Key Laboratory of Water-Sediment Sciences and Water Disaster Prevention of Hunan Province, Changsha 410114, P.R. China;

[c] College of Environmental Science and Engineering, Hunan University, Changsha 410082, P.R. China;

[d] Key Laboratory of Environment Biology and Pollution Control (Hunan University), Ministry of Education, Changsha 410082, P.R. China

[*] Corresponding author. Address: School of Hydraulic Engineering, Changsha University of Science &Technology, Changsha, 410114, PR China; College of Environmental Science and Engineering, Hunan University, Changsha 410082, P.R. China.

E-mail address: cydu@csust.edu.cn (C.Y. Du) and zgming@hnu.edu.cn (G.M.Zeng)

Abstract

Magnetic polyving akohol (PVA) immobilized the endogenous bacterium *Bacillus licheniformis* with sodium alginate to get a novel biosorbent. The optimum preparation and adsorption conditions were studied. The optimal preparation conditions was the fraction of magnetic PVA was 9%, the fraction of sodium alginate was 0.8%, the fraction of microbial suspensions was 5% and the crosslinking time was 20 h. The best adsorption conditions were listed as follows: pH was 6, the biosorbent dosage was 0.7 g L^{-1}, the initial concentration of lead ions was 200 mg L^{-1} and the optimal adsorption time was 12 h. The results of SEM and FTIR spectroscopy analysis displayed this novel biosorbents had good structure and the functional groups on the surface was abundant. The VSM analysis confirmed the novel biosorbents had good magnetic magnetization and were easily separated from aqueous medium. Under the optimum conditions, the removal rate of lead ions from waste water could reach 98%, the calculated maximum adsorption capacity could be up to 113.84 mg g^{-1}. The whole adsorption process was well fit by the pseudo-second order kinetic and it was also a Langmuir monolayer adsorption. The desorption experiments showed the biosorbent had good re-usability.

Keywords Magnetic PVA; Endophyte (*Bacillus licheniformis*); Lead ions; Biosorbent

1. Introduction

With the rapid development of mining, electroplating and lead smelting industry, the release of lead into the environment has become a serious problem (Huang et al., 2008; Zeng et al., 2013; Huang et al., 2017). Due to the non-biodegradable nature, lead can accumulate in environment and transfer in the food chains. However, even trace level of lead can pose hazards to human. Lead shows toxicity on liver, brain, nervous and reproductive system·(Tang et al., 2008; Ghosh et al., 2015; Lai et al., 2016). The main treatment of lead ions in wastewater includes physical method, chemical method and biological method (Fan et al., 2008; Hashim et al., 2011; Huang et al., 2015). Owing to the high removal rate, few secondary pollution and eco-friendly, biosorption has become an emerging field for treatment of heavy metals in recent years (Nguyen et al., 2013). The heavy metals–resistance endophytes which were extracted from hyperaccmulator have potential to adsorb heavy metals. However, the free endophytes which applied in the heavy metal adsorption are difficult to separate from water, easily lose their activity, difficult to reuse.Immobilization technology is explored to overcome above disadvantages and was utilized to separate and concentrate heavy metals from wastewater (Tuzen et al., 2007). Iron oxide magnetic nanoparticles have advantages of large specific surface area, magnetic, strong adsorption of heavy metals (Zhang et al., 2007; Xu et al., 2017; Wan et al., 2018). Iron oxide magnetic nanoparticles also can be a carrier for the microorganism immobilization to treat heavy metals polluted water and obtained a series of amazing results (Rajkumar et al., 2012; Zhang et al., 2016). Additionally, applying PVA and sodium alginate for immobilizing microorganisms to produce a new kind of biosorbent can have property of strong magnetic, easy separation, high mechanical strength

(Iqbal and Edyvean, 2004; Hu et al., 2011).

In this study, the endophytic bacterium bacterium *Bacillus licheniformis* which was extracted from *Sedum alfredii Hance* was embedded in the sodium alginate and magnetic PVA. A new kind of biosorbent was carried out. The preparation conditions and adsorption conditions were optimized. The prepared novel biosorbents was characterized by FTIR, SEM and VSM. The adsorption experiment about kinetics, isothermal model was explored in this research. At last, the reusability was also estimated.

2. Materials and methods

2.1. Materials

Biological reagents used for extracting and culturing microorganism were purchased from Aobox biotechnology Co., Ltd. (Beijing, China). All other reagents used in this research were all of analytical reagent grade and were supplied by Sinopharm Chemical Reagent Co., Ltd. (Shanghai, China). All the solutions throughout this study were prepared by ultrapure water that was from an LMO water purification system (LEAD R&D, Chongqing, China).

2.2. Isolation and culture of endophytic bacterium

The endophytic bacterium used in this study was isolated from hyperaccumulator *Sedum alfredii Hance* root, collected from Shuikoushan Mining Tailings, Hengyang, Hunan Province, China. The bacterium strains number was BRE07, the 16S rDNA sequence analysis identified result was *Bacillus licheniformis* (GenBank sequence accession No. GU967445).

The endophytic bacterium that was cultured and amplified was inculated into the seed liquid. After

incubating at 30 °C 150 rpm for 24h, the suspension was inculated to the fermentation liquid medium. Then above endophytic bacterium suspension was agitated at 150 rpm for 48h and incubated at 30 °C. All the process was operated under the sterile conditions.

2.3. Preparation of biosorbents

The entophytic bacterium *Bacillus licheniformis* was embedded within magnetic PVA and sodium alginate. The specific procedure was listed as follows. Initially, PVA was dissolved according to the proportion of 30-90 g L^{-1}, and then mixed up with iron oxide magnetic nanoparticles suspension to obtain magnetic PVA. Next, the sodium alginate was added to above magnetic PVA according to the proportion of 4-8 g L^{-1}, and then sterilized at 115 °C for 30-60 min. Then, microbe suspension was inoculated into above sterilized mixture according the proportion of 100 ml: 5-15 ml, and above mixture was added into the sterile $CaCl_2$ (0.1 M) with syringe according to the proportion of 1-3: 10. The obtained pellets was cross-linked under 4 °C for 16-24 h. Above pellets was washed twice to triple with aseptic physiological saline, and the rinsed pellets was transferred to the liquid medium shaking for 24h under 30 °C, the speed was 150 rpm. After above incubation, the pellets were washed triple with sterile ultrapure water. Finally the obtained immobilized biosorbents were utilized in adsorption of lead ions in waste water.

2.4. Orthogonal experimental design

In order to optimize the optimal preparation conditions of biosorbent, the orthogonal experiment L9 (3^4) was carried out with the removal rate of lead ions as target index. Conditions as follow, the fraction of magnetic PVA was A, the fraction of sodium alginate was B, the fraction of microbial

94 suspensions was C, cross-linked time was D. Different factors had different levels (Table S1).

95 *2.5. Physicochemical characteristics of Biosorbents*

96 The morphological and structural image of biosorbents were analyzed from environmental
97 scanning electron microscope (SEM, TESCAN MIRA 3) after gold plating at an accelerating voltage of
98 20 kV. The functional groups of biosorbents were analyzed by the Fourier transform infrared
99 spectrophotometer (FTIR, Nicolet, Nexus-670) over the range 4000-400 cm^{-1}. The VSM analysis
100 aimed to explored the magnetic properties of magnetic particles, which were assessed with a vibrating
101 sample magnetometer (Quantum Design, MPMS (SQUID) XL-7) at room temperature.

102 *2.6. Adsorption experiment*

103 Biosorbents were added into the conical flask with lead ions solution and agitated them under
104 30 °C at the speed of 150 rpm. The adsorption experiments were carried out at different Pb (II) initial
105 concentration, pH value, biosorbent dosage and time. The lead solutions were prepared with Pb
106 $(NO_3)_2.4H_2O$. The control group was set to contrast related influencing factors. The whole process was
107 under sterile conditions. All samples were treated in triplicate.

108 *2.7. Desorption experiment*

109 Biosorbents were mixed up with lead ions solution, and the solution was agitated at 30 °C for 12 h
110 by the speed of 150 rpm. The biosorbents were filtered and collected. The biosorbents were rinsed triple
111 with sterile water, and then were added into 1 M HCl solution. The desorption process was contacted
112 for 30 min at 30 °C. Then the biosorbents was filtered and collected. Above adsorption/desorption steps
113 were repeated five times.

3. Results and discussion

3.1. Optimal preparation conditions of biosorbent

The experiment was arranged under different factors and levels by the orthogonal experiments L9 (3^4). The fraction of magnetic PVA as A, the fraction of sodium alginate as B, the fraction of microbial suspensions as C and cross-linked time as D with three levels were chosen in the orthogonal experiment (Table S1). Calculate the removal rate of lead ions under different levels and factors as the target index. Then calculate K_1, K_2, K_3 to determine the optimal level. The R value reflects the effects of each factor on the adsorption.

The orthogonal experiment results (Table S2) showed the R value of different factors. The order of the effect of different factors was: the fraction of magnetic PVA (A) > the fraction of sodium alginate (B) > crosslinking time (D) > the fraction of microbial suspensions (C). The fraction of magnetic PVA had the largest effect on the removal rate. The optimum level of each factors were listed as follows: the fraction of magnetic PVA and the fraction of sodium alginate were under level 3, the fraction of microbial suspensions was under level 1, crosslinking time was under level 2. Therefore, the best preparation condition is $A_3B_3D_2C_1$. The best preparation conditions was the fraction of magnetic PVA was 9%, the fraction of sodium alginate content was 0.8%, the fraction of microbial suspensions was 5% and the crosslinking time was 20 h.

Fe_3O_4 nanoparticles were mixed up with PVA to obtain magnetic PVA. The magnetic nanoparticles showed good adsorption for heavy metal (Feng et al., 2010). The magnetic nanoparticles could increase the surface area and mechanical strength of biosorbents and was conducive to the

diffusion and adsorption of lead ions to the biosorbents (Ge et al., 2016). Magnetic PVA had large impact on the adsorption efficiency. Sodium alginate mainly affected the crosslinking establishment process of the biosorbent. Entophytic bacterium was embebbed in the biosorbent with the sodium alginate and magnetic PVA together. Hydroxyl groups that exist in sodium alginate had strong adsorption ability for lead ions. The mechanical strength, surface pore formation and growth of microbial in sphere surface were mainly affected by the crosslinking time of biosorbents (Wan Ngah and Hanafiah, 2008). The mechanical strength, microbial biomass would not be inadequate if crosslinking time was too short, the too strong mechanical strength while the crosslinking time was too long would decrease the porosity of biosorbents.

The fraction of endophytic bacterium BRE07 that embed in biosrobents had influence on the adsorption characteristics. Microorganisms that were adhered to the carrier surface were contacted with lead ions from solution firstly, and next the lead ions were adsorbed or transferred into the endophytic bacterium. When the fraction of endophytic bacterium BRE07 was too low, the space of immobilization carrier was not fully occupied, and thus the removal ability of microbial BRE07 cannot get fully utilized. However, excessive endophytic bacterium BRE07 would be occupied in the carrier and thus may lead to the endophytic bacterium inactivation (Xiao et al., 2010). Hence, appropriate fraction of endophytic bacterium BRE07 was important

3.2. Biosorption experiment

3.2.1. Effect of pH on adsorption performance

The pH value of lead ions solution affected the process of adsorption (Alkan et al., 2015). The

surface physical and chemical characteristics of biosorbents were influenced by the pH value of solution. When the pH value was low, the solution contained more H^+, and H^+ was easily binding to the biosorbents surface (Alavi et al., 2015). The biosorption site that was bond to lead ions was relatively reduced due to the binding of H^+ (Naiya et al., 2008). When the pH value was higher, the lead ions began to precipitate and $Pb(OH)^+$ was produced (Ozdes et al., 2009). Large amounts of lead ions in solution would react as insoluble oxides, hydroxide particles solution. These react would hinder the adsorption process (Saifuddin et al., 2005).

As shown in Fig.1, the adsorption rate of immobilized microorganism pellets, not immobilized microorganism pellets and microorganism were changed with the pH value. When the pH value reached 5, adsorption capacity gradually tend to be stable. When the pH was 6, the adsorption rate could achieve 95%. The adsorption process was affected by the pH because of its effects on the surface of biosorbent and surface charge.

The immobilized microorganism pellets were the endophytic bacterium BRE07 embedding in magnetic PVA and sodium alginate. The immobilized microorganism pellets had a higher level adsorption rate for lead ions. Magnetic PVA could adsorb lead ions. The endophytic bacterium BRE07 which was extracted from the hyperaccumulator *Sedum alfredii Hance* also had strong endurance and adsorption to lead ions attributing to an amount of carboxyl and hydroxyl on microbial cell surface, which could chelate, adsorb or translate lead ions. The figure indicated that the immobilized microorganism pellets had a great adsorption ability to lead ions.

3.2.2. Effect of adsorption time on performance

The adsorption time had important effect on the adsorption process (Chong et al., 2013). Normally, the adsorption process was the contact between solid and liquid boundary layer first. Then the lead ions attached on the surface of microorganisms and the biosorbents. At last the lead ions was transferred into the microorganisms or adsorbed into the biosorbents internal.

Fig. 2 is the effect of time on the adsorption. From Fig. 2, one can see the adsorption rate of immobilized microorganism pellets was much higher than microorganism. The removal rate of the lead ions was increased quickly in the first 12 h. After that, adsorption rate remained unchanged or changed very little.

The biosorption process on entophytic bacterium surface was a relatively fast stage. The proteins or small molecules that were secreted from entophytic bacteria had a chelation, complexation adsorption with lead ions (Guo et al., 2010). When the surface cell walls of entophytic bacterium were fully occupied by lead ions, the lead ions would be transferred to the internal of microbial cell. Thus the surface of biosorbent can adsorb lead ions again.

When the surface adsorption site was fully occupied, adsorption capacity achieved saturation. Then a part of lead ions were transferred into the internal space of living cells through microbial cell surface system. Another part of lead ions was transferred inside of immobilized microorganism pellets and adsorbed by the magnetic nanoparticles and calcium alginate. Therefore the biosorbent site was released and could absorb the lead ions again. This stage was relatively slow, and then the adsorption process basic gradually reached equilibrium. The results were also confirmed by the study from Xu et

al. (2013).

3.2.3. Effect of biosorbent dosage on adsorption performance

Biosorbent dosage had a greatly influence on the removal of lead ions (Boschi et al., 2011). In this experiment, the initial concentration of lead ions was 200 mg L^{-1}; the dry weight of biosorbents was 0.42-2.1 g L^{-1}. As shown in Fig. 3, with the increase of biosorbent dosage, the adsorption rate of lead ions gradually increased. When biosorbent dosage increased from 0.42 to 2.1 g L^{-1}, the removal rate increased from 70% to 98%. This phenomenon was attributed to the increase of adsorption sites on the surface of the biosorbent (O Apos Connell et al., 2008). On the other side, the concentration gradient between the adsorption sites and lead ions will increase with the increase of biosorbent dosage. The adsorption dynamic caused by different concentration gradient also increased the removal rate of lead ions. However, as the Fig. 3 shown, when the biosorbent dosage was 2.1 g L^{-1}, the removal rate of lead ions reduced to 85%. For one reason was biosorbent dosage increased the adsorption agent reunion overlap together. The overlaps lead to the available adsorption sites decreased, and thus resulting in the removal rate decline (Zhou et al., 2009). Another reason was the amount of biosorbent sites could not reach saturated with the biosorbent dosage increasing gradually. The coefficient of utilization of biosorbent decreased. Also the repulsive interactions between the adsorption sites and the enhanced electrostatic interaction resulted in the remove rate decreased (Lata et al., 2008).

3.2.4. Effect of initial ions concentration on adsorption capacity

From Fig.4, one can see the adsorption rate of lead ions was increasing when the lead ions initial concentration varied from 80 mg L^{-1} to 200 mg L^{-1}. When the lead ions initial concentration achieved

200 mg L^{-1}, the adsorption rate reached the maximum 98%. When the lead ions initial concentration was higher than 300 mg L^{-1}, the removal rate decreased gradually. As control, the adsorption rate of microorganism also changed with the lead ions initial concentration. When the initial concentration was 600 mg L^{-1}, microorganism still could adsorb lead ions. The adsorption rate of immobilized microorganism pellets were almost 4 times of free microorganism.

Normally, the concentration of lead ions had a great influence on the adsorption process (Xu et al., 2013). The adsorption capacity would increase with the increasing of the initial concentration of lead ions. When the concentration was low, the adsorption sites on the biosorbent surface were more easily to be occupied. The utilization coefficient and the removal rate would increase with the concentration. When the lead ions initial concentration was exceeded a certain limit, the biosorption sites were easily achieved to saturation. While empty binding sites decrease, the adsorption capacity would decrease (Lizama-Allende et al., 2017). On the other side, the increasing lead ions initial concentration would increase the toxicity to microorganism, and hence inhibited microorganisms' growth and metabolic activity. Eventually the exorbitant initial concentration of lead ions could inhibit the adsorption capacity of biosorbent.

3.3. Characterization of biosorbent

3.3.1. Environmental scanning electron microscope observation

In Fig. S1, (a) was the internal structure of the biosorbent, (b) was the surface structure of the biosorbent, (c) was the encapsulated magnetic particles. Fig. S1 showed the surface and interior of biosorbent was polyporous. The vesicular structure was conducive to the attachment and transform of

lead ions, and it was also conducive to endogenous bacterium adhesion. Numerous of functional groups (like hydroxyl, carboxyl, amino etc.) on the endogenous bacterium cell wall could bind to lead ions, and thus enhance adsorption ability of biosorbent (Alkan et al., 2015). Fe_3O_4 particles that were embedded in the biosorbents could enhance the stability and mechanical strength of biosorbent.

3.3.2. FTIR analysis

The biosorbents was analyzed by FTIR spectroscopy, the experimental results were shown in Fig. S2. The Fig. S2 showed that there was a characteristic peak at 441.0 cm^{-1}, which was due to the formation of Fe-O in the vibration. The results indicated the modification of magnetic nanoparticles had a certain effect on the biosorbents (Xu et al., 2012). And the characteristic peaks were found in 1196, 1495, 1814 cm^{-1}, and this phenomenon indicated the surface had the functional groups like P-O, -COOH, C=O after immobilization (Alkan et al., 2015). The characteristic peak at 3329 and 3793 cm^{-1} showed that the biosorbent surface also contained -OH and -NH functional groups (Gundogdu et al., 2009).

3.3.3. Magnetic properties

For the response ability of magnetic materials, the magnetic hysteresis loop is significant (Song et al., 2016). The magnetization of magnetic particles and pellets in this study (included Fe_3O_4, Immobilized microorganism pellets, Pellets after adsorption, Pellets after five cycles) was explored by VSM analysis. The hysteresis loops of magnetic particles and pellets (included Fe_3O_4, Immobilized microorganism pellets, Pellets after adsorption, Pellets after five cycles) at room temperature were shown in Fig. S3 (a). As presented in Fig. S3 (a), the maximum saturation magnetization of Fe_3O_4,

253 immobilized microorganism pellets, pellets after adsorption and five cycles were 63.55 emu g^{-1}, 17.03
254 emu g^{-1}, 14.69 emu g^{-1} and 6.45 emu g^{-1}. Saturation magnetizations of immobilized microorganism
255 pellets was lower than Fe_3O_4, which might be primarily ascribed to the doping of PVA and sodium
256 alginate with Fe_3O_4 nanoparticles and hence lead to the relatively decreased amount of Fe_3O_4
257 nanoparticles. The loops also displayed that the maximum saturation magnetization of pellets still could
258 achieve 14.69 emu g^{-1} and 6.45 emu g^{-1} after adsorption and five cycles. Additionally, the Fig.S3 (a)
259 indicated that there was no obvious hysteresis was found in the magnetic hysteresis loops of these
260 magnetic particles and pellets. The results confirmed that the remnant magnetization and coercivity of
261 these magnetic particles and pellets were almost zero. This phenomenon revealed that the pellets carried
262 out in this study presented strong magnetic response ability even at small applied magnetic fields. The
263 magnetic pellets that could be magnetic separated from aqueous solution were desirable for practical
264 applications.

265 *3.4. Adsorption kinetics analysis*

266 The general biosorption process has two stages, the first stage was passive adsorption (surface
267 rapid adsorption process) and the second stage was active adsorption (slow accumulation of heavy
268 metal process) (Gong et al., 2009; Sar I and Tuzen, 2009). The first stage usually occurred on the
269 surface of microbial cell wall. When the biosorbent were added into the lead ions solution, the
270 complexation reaction between the various active groups on cell wall and lead ions was completed in a
271 relatively short time. This stage was completed by adsorption, ion exchange force. Then the lead ions
272 on the cell wall were transferred to the interior of the cell (Montazer-Rahmati et al., 2011). At last the

lead ions were removed by chemical adsorption. This stage belonged to the active transport, which was relatively slow, and hence the reaction time was relatively long (Iram et al., 2010).

In this experiment, the adsorption process was fitted by the quasi first order and second order kinetic equations to analyze the adsorption kinetics. The formula used in this study was (1) and (2). The quasi first order kinetics, the quasi second order kinetic and the related parameters obtained from the experimental data was shown in the Table 1. Results shown that the first 60 min was more fitting by the quasi first order kinetics, while the R^2 values of the quasi second order kinetic were larger than the R^2 values of the quasi first order kinetic in the whole absorption process. So the whole adsorption process was more fitted by the quasi second order kinetic. All the absorption process was chemical adsorption. The same results was observed in the study that utilized *saccharomyces cerevisiae* biomass to adsorb lead (II) from aqueous solution (Ghaedi et al., 2010).

$$ln(q_e - q_t) = lnq_e - k_2 t \quad (1)$$

$$\frac{t}{q_t} = \frac{1}{k_2 q_e^2} + \frac{t}{q_e} \quad (2)$$

where q_e is the capacity of absorbed lead ions on the biosorbent at equilibrium (mg g^{-1}), the q_t is the capacity of absorbed lead ions on the biosorbent at time (mg g^{-1}), K_1 is the first-order rate constant (min^{-1}), K_2 is the pseudo-second-order rate constant (g mg^{-1} min^{-1}).

3.5. Adsorption isotherm model analysis

The experimental data was fitted by both Langmuir model and Freundlich model, and the related parameters were obtained as shown in the Table 2. The fitting equation of the Langmuir model was

292 formula (3); the fitting equation of Freundlich model was formula (4).

293 $$lnq_e = lnK_F + \frac{1}{n} \cdot lnC_e \quad (3)$$

294 $$\frac{1}{q_e} = \frac{1}{K_L \cdot q_m} \cdot \frac{1}{C_e} + \frac{1}{q_m} \quad (4)$$

295 $$R_L = \frac{1}{1 + K_L \cdot C_0} \quad (5)$$

296 where q_m is the maximum adsorption capacity (mg g^{-1}), C_e is the equilibrium concentration of lead ions
297 (mg L^{-1}), K_L is characterized as the Langmuir constant (L mg^{-1}), R_L is equilibrium constant, judge
298 reaction constant (mg g^{-1}), n is affinity constant, K_F is defined as the adsorption coefficient (Xu et al.,
299 2012);.

300 Langmuir isotherm model was used to describe the ideal situation of the surface monolayer
301 adsorption (Langmuir, 1916; Hall et al., 1966). The Freundlich isotherm model was usually used to
302 describe various suboptimal cases of surface adsorption and multi molecular layer adsorption (Gupta et
303 al., 2010). The R^2 values of both model was shown in Table 2, the R^2 values of Freundlich model was
304 lower than the R^2 values of Langmuir model. Therefore, the adsorption equilibrium can be better
305 described by Langmuir model and the maximum adsorption capacity of single molecule layer was
306 113.84 mg/g. Tabel S3 listed maximum adsorption capacities of biosorbent from this study and reported
307 in other study. The result showed that the biosorbent in this study was better than other biosorbent, and
308 prepared biosorbent was potential to apply in actual treatment.

309 *3.6. Desorption characteristics of biosorbent*

310 In order to explore the reusability of biosorbent, the adsorption-desorption experiments were
311 carried out. Experimental results (Fig. 5) showed that the removal rate of adsorption was from 98% to

312 90% after cycling five times, and the removal rate was only decreased by about 8%.The result
313 confirmed the biosorbent had a good reusability. The prepared biosorbents was promising to treat the
314 lead ions waste-water.

315 **4. Conclusion**

316 In this study, the entophytic bacteria *Bacillus licheniformis* embedding within magnetic PVA and
317 sodium alginate successfully obtained a novel biosorbent. This study showed that the adsorption
318 process was easily affected by pH, adsorption time, biosorbent dosage and initial ions concentration.
319 Under the best preparation and adsorption conditions, removal efficiency of novel biosorbent could
320 reach 98%. The SEM images showed the biosorbent had good pore structure that was beneficial to
321 adsorb lead ions. FTIR spectroscopy curves confirmed that the biosorbent had relatively stable structure
322 and abundant functional groups on surface. The VSM analysis confirmed the biosorbent could be
323 magnetic separated from aqueous solution. Equilibrium adsorption data indicated that the whole
324 process was more fitted by the pseudo second order kinetics, which was mainly ascribed to chemical
325 adsorption. According to the isothermal analysis, the adsorption process was well demonstrated by
326 Langmuir model. The calculated maximum adsorption capacity was 113.84 mg g^{-1}. The five
327 adsorption-desorption experiments showed the biosorbents had good reusability. To sum up, this novel
328 biosorbents showed a promising prospect to treat the practical heavy-metals wastewater.

329 **Acknowledgements**

330 This study was financially supported by the Program for the National Natural Science Foundation
331 of China (51109016, 51521006, 51579098, 51408206, 51308068, 51308069, 51378190), the National

Program for Support of Top–Notch Young Professionals of China (2014), the Program for New Century Excellent Talents in University (NCET-13-0186), the Program for Changjiang Scholars and Innovative Research Team in University (IRT-13R17), and Hunan Provincial Science and Technology Plan Project (No.2016RS3026), the Key Laboratory of Water Sediment Sciences and Water Disaster Prevention of Hunan Province, China (2014SS05), the Changsha science and technology program (KQ1602031).

References:

Alavi, S.A., Zilouei, H., Asadinezhad, A., 2015. Otostegia persica biomass as a new biosorbent for the removal of lead from aqueous solutions. Int. J. Environ. Sci. Te. 12, 489-498.

Alkan, H., Gul-Guven, R., Guven, K., Erdogan, S., Dogru, M., 2012. Biosorption of Cd^{2+}, Cu^{2+}, and Ni^{2+} Ions by a Thermophilic Haloalkalitolerant Bacterial Strain (KG9) Immobilized on Amberlite XAD-4. Pol. J. Environ. Stud. 24, 1903-1910..

Boschi, C., Maldonado, H., Ly, M., Guibal, E., 2011. Cd(II) biosorption using Lessonia kelps. J. Colloid Interf. Sci. 357, 487-496.

Chong, H.L.H., Chia, P.S., Ahmad, M.N., 2013. The adsorption of heavy metal by Bornean oil palm shell and its potential application as constructed wetland media. Bioresource Technol. 130, 181-186.

Fan, T., Liu, Y., Feng, B., Zeng, G., Yang, C., Zhou, M., Zhou, H., Tan, Z., Wang, X., 2008. Biosorption of cadmium(II), zinc(II) and lead(II) by Penicillium simplicissimum:Isotherms, kinetics and thermodynamics. J. Hazard. Mater. 160, 655-661.

Feng, Y., Gong, J., Zeng, G., Niu, Q., Zhang, H., Niu, C., Deng, J., Yan, M., 2010. Adsorption of Cd (II) and Zn (II) from aqueous solutions using magnetic hydroxyapatite nanoparticles as adsorbents. Chem. Eng. J. 162, 487-494.

Ge, H., Wang, C., Liu, S., Huang, Z., 2016. Synthesis of citric acid functionalized magnetic graphene oxide coated corn straw for methylene blue adsorption. Bioresource Technol. 221, 419-429.

Ghaedi, M., Ghezelbash, G.R., Marahel, F., Ehsanipour, S., Najibi, A., Soylak, M., 2010. Equilibrium, Thermodynamic, and Kinetic Studies on Lead (II) Biosorption from Aqueous Solution by Saccharomyces cerevisiae Biomass. Clean -

Soil, Air, Water 38, 877-885.

Ghosh, A., Ghosh Dastidar, M., Sreekrishnan, T.R., 2015. Recent Advances in Bioremediation of Heavy Metals and Metal Complex Dyes: Review. J. Environ. Eng., C4015003.

Gong, J., Wang, B., Zeng, G., Yang, C., Niu, C., Niu, Q., Zhou, W., Liang, Y., 2009. Removal of cationic dyes from aqueous solution using magnetic multi-wall carbon nanotube nanocomposite as adsorbent. J. Hazard. Mater. 164, 1517-1522.

Gundogdu, A., Ozdes, D., Duran, C., Bulut, V.N., Soylak, M., Senturk, H.B., 2009. Biosorption of Pb(II) ions from aqueous solution by pine bark (Pinus brutia Ten.). Chem. Eng. J. 153, 62-69.

Guo, H., Luo, S., Chen, L., Xiao, X., Xi, Q., Wei, W., Zeng, G., Liu, C., Wan, Y., Chen, J., Liu, Y., 2010. Bioremediation of heavy metals by growing hyperaccumulaor endophytic bacterium Bacillus sp. L14. Bioresource Technol. 101, 8599-8605.

Gupta, V.K., Rastogi, A., Nayak, A., 2010. Biosorption of nickel onto treated alga (Oedogonium hatei): Application of isotherm and kinetic models. J. Colloid Interf. Sci. 342, 533-539.

Hall, K.R., Eagleton, L.C., Acrivos, A., Vermeulen, T., 1966. Pore- and Solid-Diffusion Kinetics in Fixed-Bed Adsorption under Constant-Pattern Conditions. Ind. Eng. Chem. Fund. 5, 212-223.

Hashim, M.A., Mukhopadhyay, S., Sahu, J.N., Sengupta, B., 2011. Remediation technologies for heavy metal contaminated groundwater. J. Environ. Manage. 92, 2355-2388.

Hu, X., Wang, J., Liu, Y., Li, X., Zeng, G., Bao, Z., Zeng, X., Chen, A., Long, F., 2011. Adsorption of chromium (VI) by ethylenediamine-modified cross-linked magnetic chitosan resin: Isotherms, kinetics and thermodynamics. J. Hazard. Mater. 185, 306-314.

Huang, C., Zeng, G., Huang, D., Lai, C., Xu, P., Zhang, C., Cheng, M., Wan, J., Hu, L., Zhang, Y., 2017. Effect of Phanerochaete chrysosporium inoculation on bacterial community and metal stabilization in lead-contaminated agricultural waste composting. Bioresource Technol. 243, 294-303.

Huang, D., Zeng, G., Feng, C., Hu, S., Jiang, X., Tang, L., Su, F., Zhang, Y., Zeng, W., Liu, H., 2008. Degradation of Lead-Contaminated Lignocellulosic Waste by Phanerochaete Chrysosporium and the Reduction of Lead Toxicity. Environ. Sci. Technol. 42, 4946-4951.

384 Huang, D.L., Wang, R.Z., Liu, Y.G., Zeng, G.M., Lai, C., Xu, P., Lu, B.A., Xu, J.J., Wang, C., Huang, C., 2015.
385 Application of molecularly imprinted polymers in wastewater treatment: a review. Environ. Sci. Pollut. R. 22,
386 963-977.
387 Iqbal, M., Edyvean, R., 2004. Biosorption of lead, copper and zinc ions on loofa sponge immobilized biomass of
388 Phanerochaete chrysosporium. Miner. Eng. 17, 217-223.
389 Iram, M., Guo, C., Guan, Y., Ishfaq, A., Liu, H., 2010. Adsorption and magnetic removal of neutral red dye from
390 aqueous solution using Fe3O4 hollow nanospheres. J. Hazard. Mater. 181, 1039-1050.
391 Lai, C., Wang, M., Zeng, G., Liu, Y., Huang, D., Zhang, C., Wang, R., Xu, P., Cheng, M., Huang, C., Wu, H., Qin, L.,
392 2016. Synthesis of surface molecular imprinted TiO_2/graphene photocatalyst and its highly efficient photocatalytic
393 degradation of target pollutant under visible light irradiation. Appl. Surf. Sci. 390, 368-376.
394 Langmuir, I., 1916. The Constitution and fundamental properties of solids and liquids. Part I. Solid. J. Am. Chem. Soc. 38,
395 2221-2295.
396 Lata, H., Garg, V.K., Gupta, R.K., 2008. Adsorptive removal of basic dye by chemically activated Parthenium biomass:
397 equilibrium and kinetic modeling. Desalination 219, 250-261.
398 Lizama-Allende, K., Henry-Pinilla, D., Diaz-Drogett, D.E., 2017. Removal of Arsenic and Iron from Acidic Water
399 Using Zeolite and Limestone: Batch and Column Studies. Water, Air, Soil Poll. 228, 275.
400 Montazer-Rahmati, M.M., Rabbani, P., Abdolali, A., Keshtkar, A.R., 2011. Kinetics and equilibrium studies on
401 biosorption of cadmium, lead, and nickel ions from aqueous solutions by intact and chemically modified brown
402 algae. J. Hazard. Mater. 185, 401-407.
403 Naiya, T.K., Bhattacharya, A.K., Das, S.K., 2008. Adsorption of Pb (II) by sawdust and neem bark from aqueous
404 solutions. Environ. Prog. 27, 313-328.
405 Nguyen, T.A.H., Ngo, H.H., Guo, W.S., Zhang, J., Liang, S., Yue, Q.Y., Li, Q., Nguyen, T.V., 2013. Applicability of
406 agricultural waste and by-products for adsorptive removal of heavy metals from wastewater. Bioresource Technol.
407 148, 574-585.
408 O Apos Connell, D.W., Birkinshaw, C., O Apos Dwyer, T.F., 2008. Heavy metal adsorbents prepared from the
409 modification of cellulose: A review. Bioresource Technol. 99, 6709-6724.

410 Ozdes, D., Gundogdu, A., Kemer, B., Duran, C., Senturk, H.B., Soylak, M., 2009. Removal of Pb(II) ions from aqueous
411 solution by a waste mud from copper mine industry: Equilibrium, kinetic and thermodynamic study. J. Hazard.
412 Mater. 166, 1480-1487.
413 Rajkumar, M., Sandhya, S., Prasad, M.N.V., Freitas, H., 2012. Perspectives of plant-associated microbes in heavy metal
414 phytoremediation. Biotechnol. Adv. 30, 1562-1574.
415 Saifuddin, M., Kumaran, P., Others, 2005. Removal of heavy metal from industrial wastewater using chitosan coated oil
416 palm shell charcoal. Electron. J. Biotechn. 8, 43-53.
417 Sar I, A., Tuzen, M., 2009. Kinetic and equilibrium studies of biosorption of Pb (II) and Cd (II) from aqueous solution by
418 macrofungus (Amanita rubescens) biomass. J. Hazard. Mater. 164, 1004-1011.
419 Song, W., Gao, B.Y., Xu, X., Wang, F., Xue, N., Sun, S.L., Song, W.C., Jia, C.B., 2010. Adsorption of nitrate from
420 aqueous solution by magnetic amine-crosslinked biopolymer based corn stalk and its chemical regeneration property.
421 J. Hazard. Mater. 304, 280-290.
422 Tang, L., Zeng, G., Shen, G., Li, Y., Zhang, Y., Huang, D., 2008. Rapid Detection of Picloram in Agricultural Field
423 Samples Using a Disposable Immunomembrane-Based Electrochemical Sensor. Environ. Sci. Technol. 42,
424 1207-1212.
425 Tuzen, M., Uluozlu, O.D., Usta, C., Soylak, M., 2007. Biosorption of copper(II), lead(II), iron(III) and cobalt(II) on
426 Bacillus sphaericus-loaded Diaion SP-850 resin. Anal. Chim. Acta 581, 241-246.
427 Wan Ngah, W.S., Hanafiah, M.A.K.M., 2008. Removal of heavy metal ions from wastewater by chemically modified
428 plant wastes as adsorbents: A review. Bioresource Technol. 99, 3935-3948.
429 Wan, J., Zeng, G., Huang, D., Hu, L., Xu, P., Huang, C., Deng, R., Xue, W., Lai, C., Zhou, C., Zheng, K., Ren, X., Gong,
430 X., 2018. Rhamnolipid stabilized nano-chlorapatite: Synthesis and enhancement effect on Pb-and
431 Cd-immobilization in polluted sediment. J. Hazard. Mater. 343, 332-339.
432 Xiao, X., Luo, S., Zeng, G., Wei, W., Wan, Y., Chen, L., Guo, H., Cao, Z., Yang, L., Chen, J., Xi, Q., 2010. Biosorption
433 of cadmium by endophytic fungus (EF) Microsphaeropsis sp. LSE10 isolated from cadmium hyperaccumulator
434 Solanum nigrum L. Bioresource Technol. 101, 1668-1674.
435 Xu, P., Zeng, G., Huang, D., Hu, S., Feng, C., Lai, C., Zhao, M., Huang, C., Li, N., Wei, Z., Xie, G., 2013. Synthesis of

iron oxide nanoparticles and their application in Phanerochaete chrysosporium immobilization for Pb(II) removal. Colloid. Surface. A. 419, 147-155.

Xu, P., Zeng, G.M., Huang, D.L., Feng, C.L., Hu, S., Zhao, M.H., Lai, C., Wei, Z., Huang, C., Xie, G.X., Liu, Z.F., 2012. Use of iron oxide nanomaterials in wastewater treatment: A review. Sci. Total Environ. 424, 1-10.

Xu, P., Zeng, G.M., Huang, D.L., Lai, C., Zhao, M.H., Wei, Z., Li, N.J., Huang, C., Xie, G.X., 2012. Adsorption of Pb(II) by iron oxide nanoparticles immobilized Phanerochaete chrysosporium: equilibrium, kinetic, thermodynamic and mechanisms analysis. Chem. Eng. J. 203, 423-431.

Xu, P., Zeng, G.M., Huang, D.L., Yan, M., Chen, M., Lai, C., Jiang, H., Wu, H.P., Chen, G.M., Wan, J., 2017. Fabrication of reduced glutathione functionalized iron oxide nanoparticles for magnetic removal of Pb(II) from wastewater. J. Taiwan Inst. Chem. E. 71, 165-173.

Zeng, G., Chen, M., Zeng, Z., 2013. Shale gas: surface water also at risk. Nature 499, 154.

Zhang, Y., Zeng, G., Tang, L., Huang, D., Jiang, X., Chen, Y., 2007. A hydroquinone biosensor based on immobilizing laccase to modified core-shell magnetic nanoparticles supported on carbon paste electrode. Biosens. Bioelectron. 22, 2121-2126.

Zhang, Y., Zhao, Y., Chen, Y., Lu, Q., Li, M., Wang, X., Wei, Y., Xie, X., Wei, Z., 2016. A regulating method for reducing nitrogen loss based on enriched ammonia-oxidizing bacteria during composting. Bioresource Technol. 221, 276-283.

Zhou, Y., Nie, H., Branford-White, C., He, Z., Zhu, L., 2009. Removal of Cu^{2+} from aqueous solution by chitosan-coated magnetic nanoparticles modified with alpha-ketoglutaric acid. J. Colloid Interf. Sci. 330, 29-37.

1 **Tables**

4

5

6 **Table 1**

7 Kinetic parameters of the adsorption

Pseudo-first-order（first 60min）				Pseudo-second-order		
C_0	q_e	K_1	R^2	q_e	K_2	R^2
(mg L^{-1})	(mg g^{-1})	(min^{-1})		(mg g^{-1})	(g mg^1 min^{-1})	
50	25.13	0.0191	0.9781	29.85	0.0013	0.9994
100	54.08	0.0177	0.9711	59.24	0.0007	0.9991
150	77.46	0.0088	0.9141	79.72	0.0005	0.9963

Table 2

Parameters of isothermal adsorption model

Freundlich isotherm model				Langmuir isotherm model			
T	K_F	$1/n$	R^2	q_m	K_L	R_L	R^2
				(mg g^{-1})	(L mg^{-1})		
298K	14.53	0.7656	0.9648	110.41	0.0613	0.0234~0.3185	0.9804
303K	33.49	0.5517	0.9777	113.23	0.1089	0.0439~0.4787	0.9875
308K	23.60	0.7404	0.9741	113.84	0.2140	0.0754~0.6200	0.9834

Figure Captions

Fig.1. Effect of solutions pH on the adsorption. Metal concentration: 100 mg L^{-1}; biosorbent dose: 0.7 g L^{-1}; contact time: 12h.

Fig.2. Effect of contact time on the adsorption. pH value: 6; metal concentration 100 mg L^{-1}; biosorbent dose: 0.7 g L^{-1}.

Fig.3. Effect of biosorbent dosage on the adsorption. Metal concentration: 100 mg L^{-1}; pH value: 6; contact time: 12 h.

Fig.4. Effect of initial concentration on the adsorption. Biosorbent dosage: 0.7 g L^{-1}; contact time: 12 h; pH value: 6.

Fig.5. Five consecutive adsorption-desorption cycles of immobilized microorganism pellets for Lead ions. Metal concentration: 200 mg L^{-1}; biosorbent dosage: 0.7 g L^{-1}, contact time: 12h; pH value: 6.

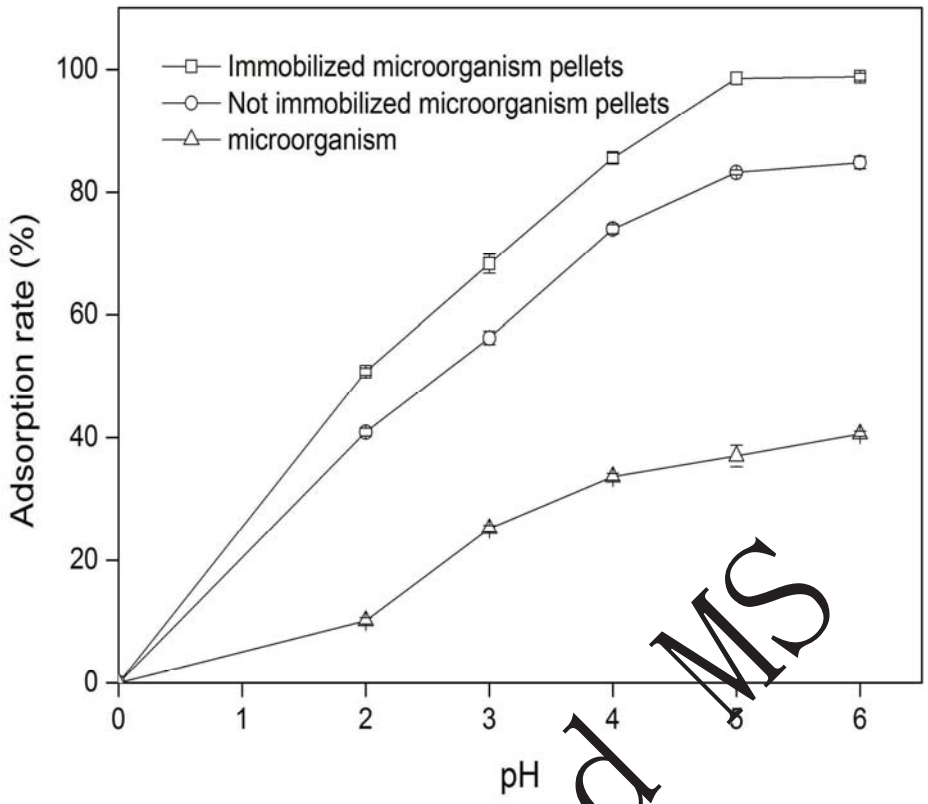

14

15 **Fig.1.** Effect of solutions pH on the adsorption. Metal concentration: 100 mg L^{-1};

16 biosorbent dose: 0.7 g L^{-1}; contact time: 12h.

17

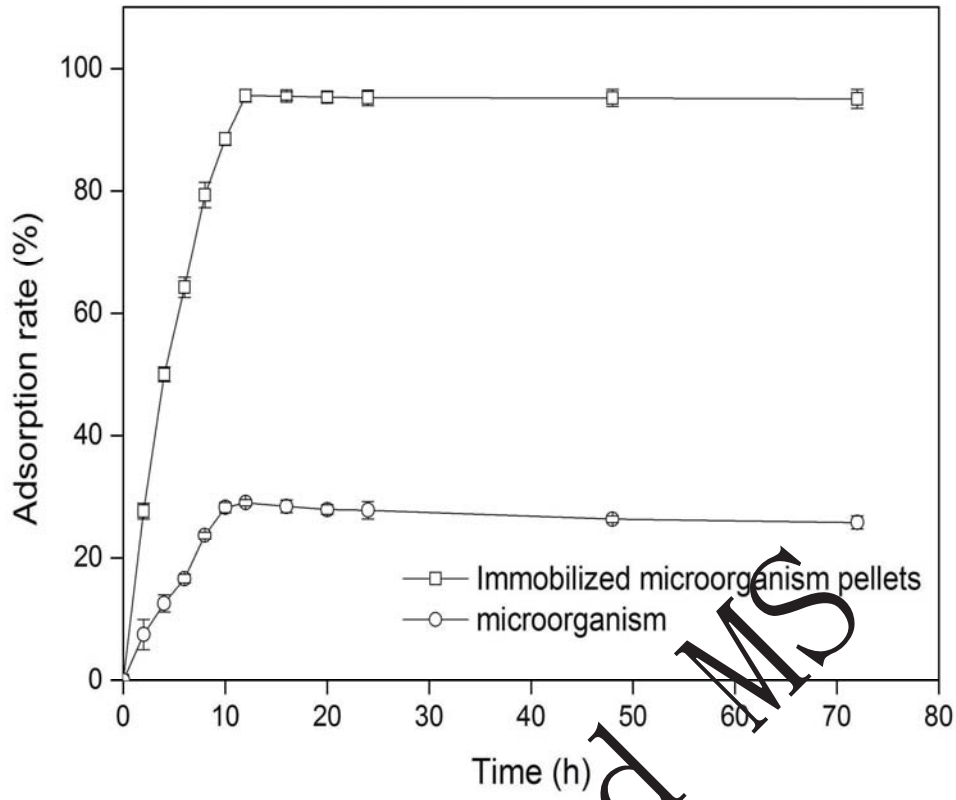

Fig.2. Effect of contact time on the adsorption. pH value: 6; metal concentration 100 mg L^{-1}; biosorbent dose: 0.7 g L^{-1}.

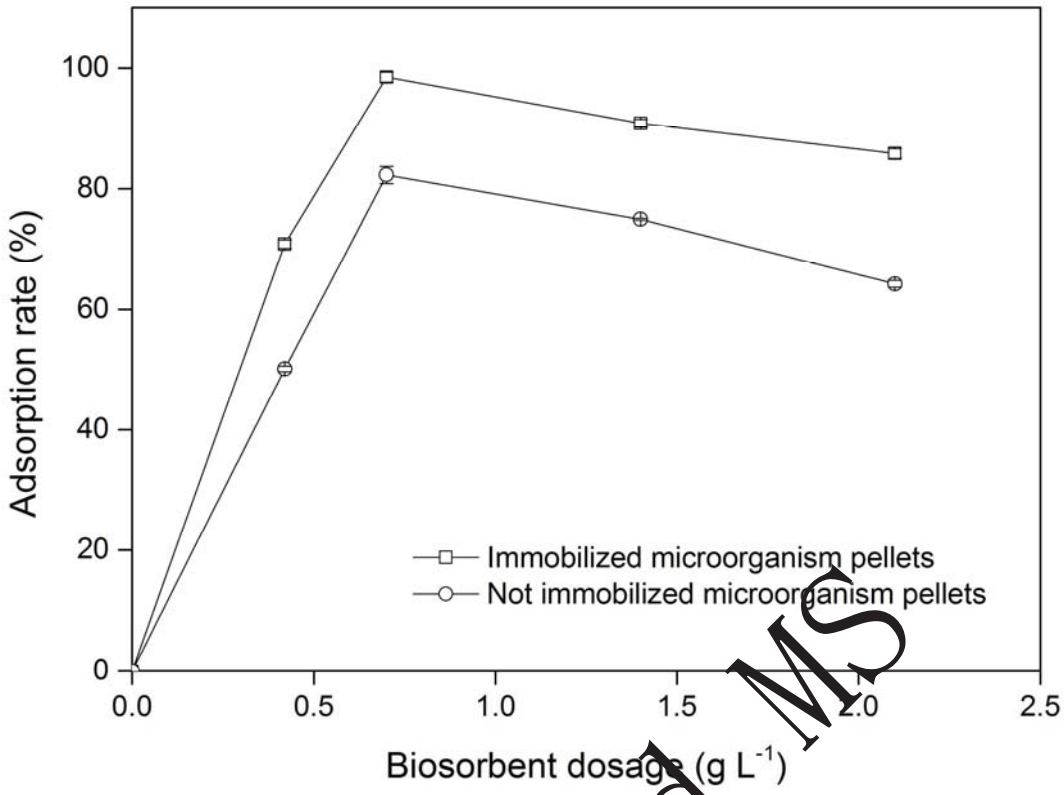

21

22 **Fig.3.** Effect of biosorbent dosage on the adsorption. Metal concentration: 100 mg L^{-1};

23 pH value: 6; contact time: 12 h.

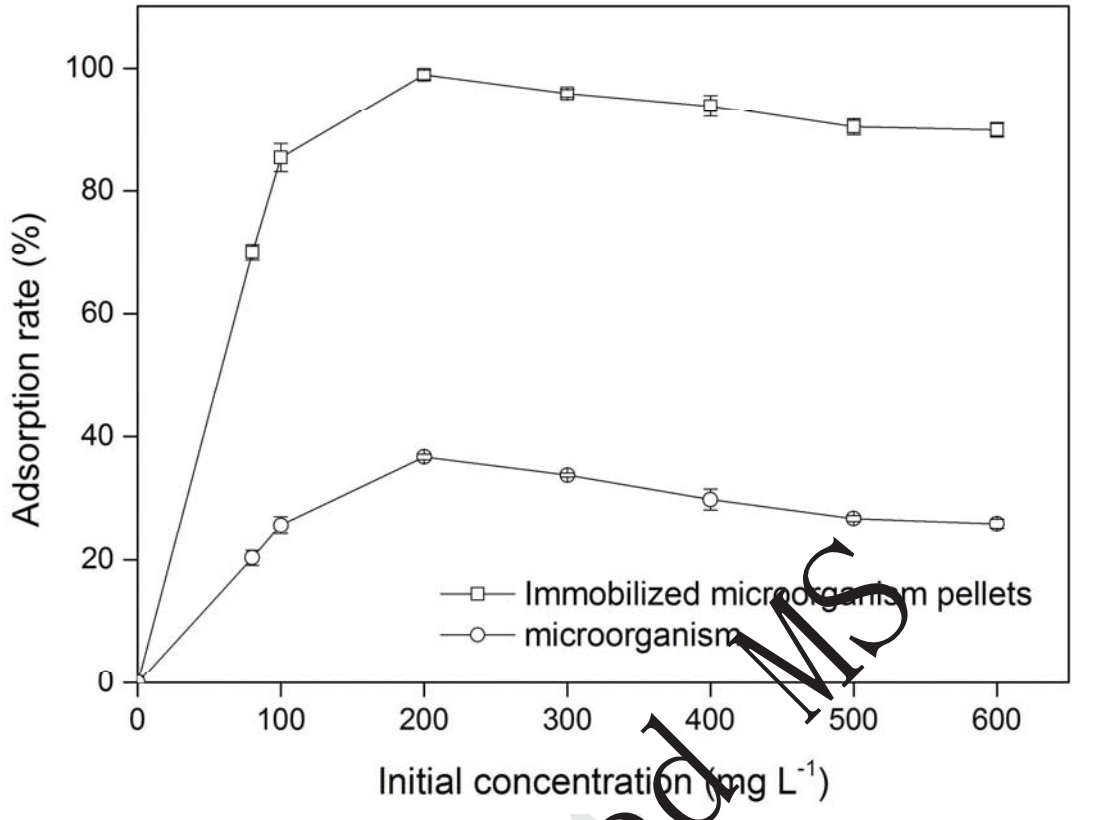

Fig.4. Effect of initial concentration on the adsorption. Biosorbent dosage: 0.7 g L^{-1}; contact time: 12 h; pH value: 6.

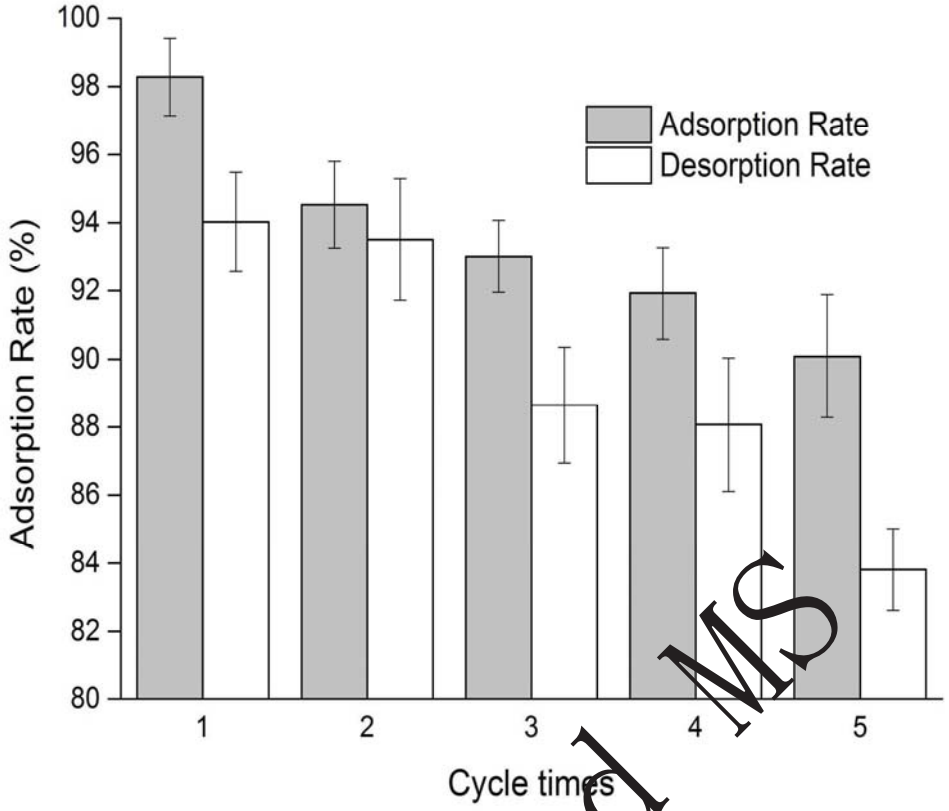

27

28 **Fig.5.** Five consecutive adsorption-desorption cycles of Immobilized microorganism

29 pellets for Lead ions. Metal concentration: 200 mg L^{-1}; biosorbent dosage: 0.7 g L^{-1},

30 contact time: 12h; pH value: 6.

Highlights

- A novel biosorbent: magnetic polyvinyl alcohol immobilized the entophytic bacteria *Bacillus licheniformis* was prepared.
- Optimum prepared conditions were explored as the fraction of magnetic polyvinyl alcohol, the crosslinking time, etc.
- Optimum biosorption conditions were studied as the pH of solution, the adsorbent dosage, etc.
- Pseudo-second-order and Langmuir models best described the lead ions adsorption.
- The biosorbents had large capacity for lead ions removal, high separability from solutions and good re-usability.